LETTER OF INTENT

Primakoff Production of Hyperon Excited States

M. V. Hynes*, R. L. Burman, A. L. Hallin, C. M. Hoffman,
D. W. MacArthur, and V. D. Sandberg
Los Alamos National Laboratory

G. Igo, C. Newsom, G. Pauletta, and C. W. Wong
University of Calilfornia at Los Angeles

ABSTRACT

Electromagnetic decays have served as bench marks in the developing stages of the shell model in nuclei. The quark confinement pictures for baryons are now in a similar developing stage. These experiments will test in an unambiguous way, the quark configurations present in the low-lying excited states of the Λ, Σ, and Ξ by measuring the electromagnetic branching ratios that connect them. Experimentally, most of the decays can be measured at FNAL using the hyperon beam via the Primakoff effect. We specifically propose to measure first the Primakoff excitation of $\Sigma^- \rightarrow \Sigma^{-*}(1385)$. This electromagnetic transition is forbidden in SU(3) by U-spin conservation but is allowed in SU(6) with massive quarks. It is also particularly sensitive to two-body corrections for magnetic dipole moments and will provide a crucial test of these models.

*Spokesman: MP-4, MS H846
Los Alamos, NM 87545
(505) 667-6909
(505) 667-6941

I. INTRODUCTION

This series of experiments will measure the electromagnetic branching ratios that connect the ground and low-lying excited states of the Λ, Σ, and Ξ hyperons. Through such a measurement it is possible to make an unambiguous test of quark wave functions for these states. The lack of ambiguity arises from our certain knowledge of the operator mediating the transition, i.e., it is electromagnetic. The only uncertainty that remains in a measurement of the radiative width arises from the wave functions.

The planning for this series of experiments has stimulated a number of theoretical groups to calculate the radiative widths of interest here. Groups at MIT (E. Moniz), Los Alamos (L. Heller, J. Johnstone), UCLA (C. W. Wong), and York University (R. Koniuk) are actively involved. Each of the various quark confinement model calculations available to our group make very different predictions for these radiative widths. A definitive measurement can serve to help direct the further development of these models.

We propose in this letter of intent to carry out this series of experiments in three phases using negative, positive, and neutral hyperon beams. This document discusses both the general physics motivation and feasibility for our experiments and presents in detail our plans for measuring the electromagnetic excitation of the $\Sigma^- \rightarrow \Sigma^{-*}(1385)$ transition. For the reader's convenience each major section to follow starts with a section that discusses this specific measurement.

II. PHYSICS BACKGROUND

A. The $\Sigma^- \rightarrow \Sigma^{-*}(1385)$ Transition

The simple three-quark (q^3) model for the Σ^- ground state has the two light quarks (two d's) coupled to S = 1, T = 1, and the strange quark jacknifed against this configuration to give $J^\pi = \frac{1}{2}^+$. All quarks are in the S-state as shown in Fig. 2. The $\Sigma^{-*}(1385)$ configuration in this model also has all quarks in the S-state but with all spins aligned giving $J^\pi = \frac{3}{2}^+$ (Fig. 2). Thus in this model the electromagnetic transition connecting these two states is pure magnetic dipole (M1). The magnetic

dipole moment for this transition can be calculated in the same way as for ground state magnetic moments with the result that

$$M1(\Sigma^{-*} \rightarrow \Sigma^{-}\gamma) = \frac{2\sqrt{2}}{3}(\mu_s - \mu_d)$$

where $\mu_s(\mu_d)$ is the magnetic moment of the strange (down) quark.

This transition in pure SU(3) is forbidden. This due to the equality of quark masses in the absence of symmetry breaking and the equality of the charges for the strange and down quarks. This evidently makes the magnetic moments for the strange and down quarks equal and hence the above expression vanishes. Seen in another way, this electromagnetic transition is forbidden by U-spin conservation. The Σ^- group state is in a U-spin doublet while the excited state Σ^{-*} is in a U-spin quartet (Fig. 6). Because the photon transforms as a U-spin singlet it cannot couple a doublet to a quartet.

In broken SU(3) or SU(6) with massive quarks, U-spin is no longer a conserved quantity and quarks do not have the same masses. Hence the transition dipole moment above does not vanish and can be related to already measured ground state magnetic moments.

$$MI(\Sigma^{-*} \rightarrow \Sigma^{-}) = \frac{1}{\sqrt{2}}(\mu_\Lambda - \mu_{\Sigma^-})$$

The above relationship yields a radiative width of 3.7 ± 0.4 keV.

The simple q^3 model has not had great success in describing the ground state magnetic moments of the baryons. As a result, considerable work has been done of late on corrections to this model arising from, for example, pion cloud contributions. Recent work by Brown, Rho and Vento[19] indicates that these corrections reduce the effective magnetic moment of the down quark thus forcing it closer to the magnetic moment of the strange quark. In the context of this model the effective magnetic moment of the down quark can equal that of the strange quark. The authors of this work did not calculate the transition moment that we propose to measure. However,

they do observe that a measurement sensitive to the difference between the down and strange quark would provide a crucial test of these corrections.

The S-state configuration of the quarks in the simple q^3 model was first questioned by Lipkin.[20] The possibility of mixing an L = 2 decaplet into the conventional L = 0 octet is proposed in this work as remedy for some of the shortcomings of SU(6). The situation is likened to the D-state admixture in the deuteron. Admixture of L = 2 components in the SU(6) decaplet is also discussed. For the $\Sigma^-(\frac{1}{2}^+) \rightarrow \Sigma^{-*}(\frac{3}{2}^+)$ transition we propose to measure, an electric quadrupole (E2) component is allowed in addition to the M1 component already discussed. In order for the E2 component not to vanish, an orbital quantum number must change by two units. Thus, the presence of an E2 component in the transition will be a clear signature of L = 2 admixtures in the conventional SU(6) L = 0 descriptions of these states. Because the Σ^- beam at FNAL can be produced with a high degree of polarization, a measurement of the spin transfer from Σ^- to Σ^{-*} states is possible. This measurement can uniquely determine whether the exchanged photon was M1 or E2 in nature, thus providing a measurement of possible L = 2 admixtures.

B. General

The spectrum of hyperon states of interest in these experiments are shown in Fig. 1. Unlike the S = 0 resonances there are isoscalar (Λ) and isovector (Σ, Ξ) states. A principle difference between the S = 0 and S = -1, -2 resonances lies in their total decay widths. For the N and Δ resonances typical widths are about 100-200 MeV. Conversely, the widths for the Λ, Σ, and Ξ resonances are about an order of magnitude smaller $\Gamma \approx$ 10-40 MeV. The $\Lambda^*(1520)$, the first S = -1 resonance above K^-P threshold, has a width of 15.5 ± 1.5 MeV.

The very narrow widths of the S = -1, -2 resonances make them ideal candidates for the study of radiative decays because of the experimentally favorable signal-to-noise ratio and their isolation from neighboring states.

The remaining S = -1 resonances of interest here, $\Lambda^*(1405)$ $1/2^-$ and $\Sigma^*(1385)$ $3/2^+$ both lie below K^-P threshold with widths of about 40 MeV. These resonances are known to play an important role in K^-P radiative

capture reactions but a detailed knowledge of their electromagnetic properties is lacking.

The S =-2 resonances of interest here, the $\Xi(1321)1/2^+$ and $\Xi^*(1530)3/2^+$, are each in an isospin doublet. Electromagnetic decay of the Ξ^* can only connect it to the Ξ ground state (Fig. 1). Electroweak decays of the Ξ and Ξ^* will connect to the S = -1 resonances and although of intrinsic interest for other reasons they will not be discussed here.

The properties of these hyperon excited states, including the principle decay modes, are listed in Table I.

C. The Quark Model

A simple three-quark model (q^3) for the ground state Λ, Σ and Ξ have up, down and strange quarks in the S1/2 orbit. The light quarks (up and down) are coupled to total spin-isospin S = 0, T = 0 for the Λ and to S = 1, T = 1 for the Σ as displayed in Fig. 2. The remaining S = -1 even-parity state, the $\Sigma^*(1385)3/2^+$ has the strange quark spin aligned with the S = 1, T = 1 light quarks (Fig. 2). The ground and excited states of the Ξ have two strange quarks in the S1/2 orbit coupled to S = 1 as shown in Fig. 3. For the ground state the remaining light quark is in the S1/2 orbit coupled to give S = 1/2, T = 1/2 while for the excited state it is coupled to give S = 3/2, T = 1/2.

The odd parity states, the $\Lambda^*(1405)1/2^-$ and $\Lambda^*(1520)3/2^-$ have one quark in the P1/2 and P3/2 orbits respectively. DeGrand and Jaffe[1] have pointed out that the kinetic energy for the $1/2^-$ state is considerably lower if the strange quark is placed in the P1/2 level rather than one of the light quarks. Thus the q^3 S1/2 configuration for the $\Lambda^*(1405)1/2^-$ state consists of the light quarks in S1/2 coupled to S = 0, T = 0 and the strange quark in the P1/2 orbit as shown in Fig. 4. This configuration requires that any radiative transition from this state is a pure strange quark P1/2 → S1/2 transition. Because the electromagnetic operators can change the quantum numbers of only one particle, the radiative widths for $\Lambda^*(1405) \rightarrow \Sigma(1193)$,or $\Sigma^*(1385)$ are strictly zero.

The simplest q^3 configuration assumption for the $\Lambda^*(1520)3/2^-$ has the strange quark in the P3/2 state with the light quarks coupled to S = 0, T = 0. However, gluon exchange calculations by DeGrand[4] and others indicate a sizeable admixture of light quark occupation in the P3/2 orbit

with the remaining quarks in S1/2 coupled to $S = 0$, $T = 0$, as shown in Fig. 4. In the notation of DeGrand the $\Lambda^*(1520)3/2^-$ wave function is written as

$$\Lambda^*(1520)3/2^- = a\ {}^4\underline{8} + b\ {}^2\underline{8} + c\ {}^2\underline{1} \qquad |a|^2 + |b|^2 + |c|^2 = 1 \ ,$$

where ${}^{2S+1}\underline{\sigma}$ means the SU(3) flavor multiplet σ with total spin S. DeGrand finds $c = 0.85$, $b = -0.51$, $a = 0.1$, indicating a predominance of singlet and octet configurations as already discussed. The ${}^4\underline{8}$ component corresponds to having one quark in the P1/2 orbit, the two S-state quarks coupled to $S = 1$ and the system coupled to $3/2^-$. Other gluon exchange calculations find similar admixture coefficients with however smaller ${}^4\underline{8}$ contributions. Ignoring the small ${}^4\underline{8}$ admixtures, the wave function is as shown in Fig. 5. This configuration and the one-body nature of the electromagnetic operators implies that the radiative width for the transition $\Lambda^*(1520) \to \Sigma^*(1385)$ is zero. We have therefore in the pure q^3 model three forbidden radiative transitions $\Lambda^*(1405) \to \Sigma^*(1193)$, $\Sigma^*(1385)$ and $\Lambda^*(1520) \to \Sigma^*(1385)$ due to this effect.

There is an additional selection rule that enters for some of the transitions of interest here. The SU(3) classification scheme places the ground state Σ and Ξ in the $1/2^+$ baryon octet whereas their first excited states, $\Sigma^*(1385)$ and $\Xi^*(1530)$ are members of the $3/2^+$ baryon decaplet as displayed in Fig. 6. In this figure t_3 is plotted versus hypercharge with I-spin, U-spin and V-spin axes as shown. In pure SU(3) I and U-spin are invariants. Thus the Σ^{*-} and Ξ^{*-} being in a U-spin quarted cannot decay through a U-spin scalar interaction to their respective ground states which are in a U-spin doublet. The photon transforms as a U-spin scalar and thus the electromagnetic decay of these states to their ground states is forbidden. In contrast, the electromagnetic decays of the Σ^{*o}, Σ^{*+} and Ξ^{*o} to their respective ground states do not violate U-spin and are thus allowed.

SU(3) is of course a broken symmetry and it is precisely the symmetry breaking that splits the masses of the members of a multiplet. Thus when the constituent quarks are allowed to have different masses, the strange quark being heavier than the non strange ones, the forbidden transitions

just cited become allowed. The electromagnetic transition amplitudes will be proportional to the difference between the strange and non strange quark masses.

The remaining allowed widths can be calculated straight forwardly from the quark wave functions:

$$W_\gamma = 2k \frac{1}{2S_i + 1} \sum_{\substack{m_i\, m_f \\ \lambda = \pm 1}} \left| \langle f, m_f | \int d\underset{\sim}{r}\, \hat{\underset{\sim}{\varepsilon}}_{k\lambda} \cdot \underset{\sim}{J} e^{-i\underset{\sim}{k}\cdot\underset{\sim}{r}} | i, m_i \rangle \right|^2 \Bigg|$$

$$\hat{\underset{\sim}{\varepsilon}}_{k\lambda} \cdot \underset{\sim}{k} = 0, \quad \lambda = \pm 1 \quad .$$

In this expression the current operator is given by

$$\underset{\sim}{J} = e_f \psi^+ \underset{\sim}{\alpha} \psi \quad ,$$

with e_f the charge of the quark with flavor f, $\underset{\sim}{k}$ is the photon momentum and $\psi(\psi^+)$ is the initial (final) quark wave function and α is the usual electromagnetic propagator. Moniz, Soyeur and Kaxiras* have calculated the allowed radiative widths for the neutral S = -1 states in the context of the fixed radius, static cavity approximation to the MIT bag model. Their results for the pure q^3 wave functions are listed in Table II. Also in this table are listed the results of T. Kaxiras** who has calculated these widths in the context of the Isgur-Karl(IK) model.[3] In this model two sets of basis states were used. In the "SU(6)" basis the spin-isospin wavefunctions are symmetrized in all three quarks and they are given in the limit of equal masses. The transition widths are calculated however, with differing quark masses. In the "uds" basis the wave functions are symmetrized only with respect to the u and d quarks. The strange and non-strange quark masses are treated as before. The results in these two cases are listed in the appropriate columns in the table. Evidently the three different predictions differ by as much as a factor of 60. In

*E. Moniz, M. Soyeur and T. Kaxiras, private communication.
**T. Kaxiras, private communication.

addition, some of the transitions forbidden in the MIT bag are allowed in the IK model. The constituent quark model (CQ) results are also shown.

The assumption of pure q^3 configurations for these states has recently been brought into question by Mulders* who calculated the importance of $q^4\bar{q}$ admixtures for the $\Lambda^*(1405)$. In this work the quarks for the $q^4\bar{q}$ configuration were taken to be in the S1/2 orbit and the q^3 configuration was taken to be as in Fig. 4. Using a simple two state mixing model, an estimate of the relative strengths was obtained:

$$\Lambda^*(1405) = 0.8\ |q^4\bar{q}\rangle \pm 0.6|q^3\rangle$$

Such a large $q^4\bar{q}$ admixture for the $\Lambda(1405)$ considerably alters the results listed in Table II. In particular the $\Lambda^*(1405) \to \Sigma$ transition rates are no longer zero. Moniz and Soyeur have calculated the effect of including these $q^4\bar{q}$ admixtures on the radiative widths by using the results of Strottman for the $q^4\bar{q}$ components in the Λ and Σ ground states[4]. These results and their estimates for such admixtures in the $\Lambda^*(1520)$ state are listed in Table III. Since the relative phase of the $q^4\bar{q}$ and q^3 contributions is not known, the table displays the results for constructive and destructive interference. The $\Lambda^*(1405)$ radiative decay to the Σ ground state has no q^3 component and goes only through the $q^4\bar{q}$ admixtures.

The low lying excited states of the S = -1,-2 baryons provides a very useful laboratory in which to study quark confinement models. The spectrum includes both positive and negative parity states. The positive parity states and their interconnecting transitions allows for tests of the S-state wavefunctions and quark magnetic moments. In addition they may allow for tests of possible quadrupole deformations through the presence of E2 components in the transitions. The negative parity states and their transitions provide a different test of quark wave functions, one in which the orbital quantum number of at least quark must be changed. An experimental determination of these radiative transition widths will shed considerable light on the quark structure of these states in particular,

*P. Mulders, private communication.

and can help to direct the development of quark confinement models in general.

D. Existing Measurements

The available electromagnetic data on the states of interest here is quite sparse. The $\Sigma^{0*}(1193)$ decays 100% to $\Lambda(1116)\gamma$ and has been measured by Dydak et al.[5] to be 11.5 ± 2.6 keV. In this experiment a 20-GeV Λ beam at the CERN SPS was incident on a Uranium target. The Primakoff effect was used to produce Σ^0's in the inverse reaction $\Lambda + \gamma \rightarrow \Sigma^0$. This value does not compare well with the MIT bag model calculation which predicts 4.5 keV or about four times smaller. This is not too surprising since the same model predicts 255 keV for the $\Delta \rightarrow N\gamma$ radiative width while the experimental value is 630 keV. The reasons for these discrepancies are not understood. The static bag approximation neglects recoil which will alter the theoretical predictions but no estimate of the changed values is available. The IK model prediction, 8.4 and 8.8 keV are about 20% low for this transition. While the CQ estimate comes very close with 12.1.

There exists one measurement of the $\Lambda^*(1520) \rightarrow \Lambda^*(1115)\gamma$.[6] However, in order to obtain the radiative width, an appreciable $\Sigma^0\gamma$ background subtraction was made assuming that the $\Lambda(1520)$ is an SU(3) singlet. Such a model dependent subtraction severely compromises the utility of this measurement. Lastly, there are upper bounds on the $\Sigma^*(1385)$ radiative decay widths.[7]

III. EXPERIMENTAL CONSIDERATIONS

A. Primakoff Excitation of the $\Sigma^{-*}(1385)$

The Primakoff effect[8] will be used to electromagnetically excite a ground state Σ^- beam incident on a high Z target. The production cross section for the $\Sigma^{-*}(1395)$ via this process depends directly on the electromagnetic width for these state. Using the different quark model predictions available to our group this cross section has been calculated and is shown in Fig. 10. The predictions differ by a factor of 2. The chiral bag model calculation is expected to be significantly different than these.

In order to identify the electromagnetic production from other strong production processes both the invariant mass and vector momentum for the excited final state particle needs to be measured. The strong production processes are small at t = 0 and decrease slowly with increasing t while the electromagnetic production is large at t = 0 and decreases rapidly with t. A measurement of the production cross section as a function of t thus provides an unambiguous signature of the production mechanism.

Table IV lists the experimental parameters that are used in a count rate estimate for the Σ^{-*} electromagnetic process. An average of the different quark model predictions for the electromagnetic width of this transition is used in this estimate along with an 0.10 interaction length uranium target. The final state Σ^{-*} delays 88% to Λ^- which yields $p\pi^-\pi^-$ 56% of the time. The incident Σ^- beam momentum is chosen to be 250 GeV/c where the recent flux measurements of E497 have been used. Assuming the parameters as listed in the table and at 400 GeV/c primary proton production beam with 5000 spills per day yields an event rate of 600 events/day for the transition of interest. Because the Primakoff production cross section rises with increasing hyperon energies our group anticipates no major difficulties in running with a tevatron-like primary proton beam. This point is currently under detailed study.

The final state signature for the Σ^{-*} will be $\Lambda\pi^- \rightarrow p\pi^-\pi^-$. In-beam Ξ^- decay 100% to $\Lambda\pi^-$ and hence mimics this signature. The mass difference of ~60 MeV between Ξ^- and Σ^{-*} allows for an easy identification of the final state in off line analysis. However, on-line the in-beam Ξ^- present a trigger rate problem. Because the Ξ^- will delay any where along the beam line while the Σ^{-*} will delay immediately after production in the target, it is possible to resolve this problem by requiring that the prompt π^- come from the Primakoff target. By requiring in addition that this π^- emerge at an angle greater than the divergence of the beam eliminates all in-beam particles while sacrificing only ~0.5% of the Σ^{-*} events. The hardware for implementing this measurement exists at the hyperon channel. The fast electronics and logic needed to include this decision in the trigger is under developement.

Another source of background for the $\Lambda\pi^-$ final state signature arises from diffractive dissociation of the Σ^- on a heavy nucleus.[21] A measurement of this process was made at BNL using a 24 GeV/c Σ^- beam.[22]

This work reports no Σ^{-*} production and set an upper limit on this strong production background. At higher energies this process is theoretically predicted to be slightly smaller while the experimental evidence is that it decreases rapidly with increasing energy. Assuming a slight decrease at the 250 GeV/c hyperon energy we have selected for this experiment, the total cross section ratio of Primakoff production versus diffractive dissociation is about 1/3. This ratio of course reflects an intergration of these processes for all t. Near t = 0, the production process is completely dominated by Primakoff production.

The standard hyperon apparatus already available at the hyperon channel will be used for momentum determination and track reconstruction.

Our planning for the measurement of the spin transfer for $\Sigma^- \rightarrow \Sigma^{-*}$, which is sensitive to the L = 2 admixtures, is in its beginning stages. The existing apparatus is sufficient for determining all decay planes and hence Λ polarization. We will await a completion of our detailed study for a beam time estimate for this experiment.

B. Primakoff Production of S = 1,-2 Excited States

The Primakoff effect[8] is a well established technique for studing electromagnetic decay rates. In this approach, sometimes referred to as the virtual photon target technique, a high energy beam of ground state particles is incident on a high Z nucleus as shown in Figure 7. The beam particle picks up a virtual photon from the Coulomb field of the nucleus and leaves this vicinity in one of its excited states. In order to identify this electromagnetic production mechanism from other strong production processes, the full four vector (invariant mass and vector momentum) needs to be measured for the excited final state particle. The strong production processes are small at t = 0 and decrease very slowly with increasing t. The Primakoff production has a sharp maximum very near t = 0 and falls off quickly with increasing t. Thus after determination of the invariant mass of the excited final state, a measurement of its production angle provides an unambiguous signature of the production mechanism.

The Primakoff effect has been used to measure the lifetimes of the π^0[9] and η[10] mesons and recently at FNAL to measure the electromagnetic widths of the ρ^-[11], $K^{*-}(890)$[12], $K^{*+}(1430)$[13] and A2(1310)[14] mesons. The only application of this technique to baryons is from Dydak et al.[15] who measured the Σ^0 lifetime at CERN by coulombically exciting an Λ^0 beam incident on a uranium target. This lifetime recently has been remeasured at the FNAL hyperon channel in experiment #619 (T. Devlin, spokesman) to much higher precision (~1%). The precision of this new measurement is made possible by the much higher hyperon momenta at FNAL (100-300 GeV/c). The higher momenta allows for three important improvements over the earlier measurement. First, the Primakoff production is greater at higher momenta. Second, the competing strong processes are smaller. Third, the corrections to the Primakoff production due to nuclear absorbtion[16] are at the 10% level instead of 30% as for the the earlier measurement (made at 5-20 GeV/c). Going to still higher hyperon momenta introduces an undesirable additional correction due to electron screening of the nuclear charge distribution.[16] Thus the momenta range of 100-300 GeV/c is about optimum for Primakoff studies.

Of the thirteen possible electromagnetic transitions of interest in this program of experiments eight are in principle measureable at the FNAL hyperon beam facility. These are shown in Figure 8. The excluded transitions would involve either beams of excited hyperons or of Σ^0's which are of course nowhere available.

The results of a calculation of the Primakoff production total cross sections in millibarns using the various confinement predictions for the radiative widths listed in Table II, are shown in Figures 9 and 10. This calculation uses the formalism developed by Faldt[16] where nuclear absorbition is approximately taken into account. The Coulomb distortions for the charged hyperon beam transitions are expected to be small at FNAL energies[16] and have not been included. The final analysis of the data from these experiments will of course include a far more precise treatment of all these effects[17]. An incident hyperon beam momentum of 250 GeV/c was selected for all these transitions so as to keep these corrections at the 10% level.

Figure 9 displays these results for the four transitions requiring the neutral hyperon beam where the already measured (E619) $\Lambda^0\gamma \to \Sigma^0$ cross section is shown for comparison. All of the transitions shown are on the average only about 1.5 to 5 times smaller than this already complete high precision (~1%) result. For the first transitions shown the different model predictions differ by a factor of two while for the last all models nearly agree. These transition are both $1/2^+ \to 3/2^+$ or octet to decuplet transitions where the quarks are in the S state. Model predictions should agree about as well as they do for the magnetic dipole moments of the ground states. For the two transition in the middle involving excitation of negative parity states model predictions vary by as much as a factor of 100. For these transitions the orbital quantum number of at least one of the quarks must change by one unit. The configurations that the different models use to accomplish this while keeping the excited state spectrum the same gives rise to these very different results.

Figure 10 displays the total Primakoff cross sections for those transitions requiring the charged hyperon beams. These transitions are all of the octet to decuplet type and the same factor of two differences encountered earlier obtains.

C. Production Rate Estimates

Estimates of Primakoff production rates for the transitions of interest are listed in Table IV. The choice of final state signature for each transition has been made on the basis of its branching ratio and uniqueness given other competing processes in the beam. A more complete Monte Carlo study of these background processes is in progress. For those transitions with only charged particles in the final state, the uranium target thickness is chosen to be 0.10 interaction lengths so that these particles will exit the target with little attenuation. For those transitions with photons in the final state, a thinner 0.03 interaction length target is chosen to keep photon losses small. Finally the flux of hyperons per pulse is derived for 250 GeV/c incident momentum from the most recent hyperon flux measurements[18] and 5000 spills per day is assumed.

Evidently, the event rate for six of the seven transitions listed is in the range of 100 to 1000 per day. The preliminary background estimates indicate a ten-to-one or better signal-to-noise ratio for these six

transitions for t near zero indicating the relative ease with which the measurements can be made.

D. Survey of Existing Data

While no experiment in has ever looked for the transitions discussed here, it is possible that the neutral beam transition signatures satisfied the trigger requirements for E619. The tapes for this experiment are currently being scanned for these signatures and for backgrounds that would interfere with a future measurement.

In addition, two tapes of data for the negative hyperon beam incident on a polyethelene brick (0.10 interaction lengths) were taken a couple years ago and are being analyzed now for relevant backgrounds. No Primakoff events are expected to be on these tapes due to the rather small number of radiation lengths (0.18) this target thickness represents.

E. Experimental Equipment

For the measurement of $\Sigma^- \to \Sigma^{-*}$ we anticipate no major additions to the already existing hyperon channel detector system. A hard wired logic system for the trigger selection will be developed by our group. Because this is a relatively standard vertex trigger problem that has been addressed by several other groups in different contexts we anticipate no significant obstacles. For Tevatron operations it may be necessary to build a new central channel for the existing hyperon magnet in order to extract higher energy hyperons. In addition, the existing beam defining chambers will probably have to be replaced with higher accuracy devices such as silicon strip detectors. It is however possible that we can run at 350 GeV/c Σ^- hyperon momenta with a 1 TeV primary production beam. The beam characteristics are unknown in detail at present. These issues will be discussed in our forthcoming proposal. We at this time anticipate no major conflicts between our experiment and Tevatron operations.

F. Personnel

At present the collaboration for this experiment is still being formed. Commitments have been made by the following:

Los Alamos National Laboratory

M. V. Hynes

R. L. Burman
A. L. Hallin
C. M. Hoffman
D. W. MacArthur
V. D. Sandberg

University of California at Los Angeles

G. Igo
C. Newsom
G. Pauletta
C. W. Wong

We are in contact with the collaborators for E715 (Precision Measurement of the Decay of $\Sigma^- \to ne^-\nu$, P. Cooper, Spokesman). These workers are favorably disposed towards collaborating with us on the $\Sigma^- \to \Sigma^{-*}$ measurement.

REFERENCES

1. T. DeGrand and R. L. Jaffe, Ann. of Phys., 100, 425 (1976).
2. T. DeGrand, Ann. of Phys., 101, 496 (1976).
3. R. Koniuk and N. Isgur, Phys. Rev. D21, 1868 (1980); and K. T. Chad, N. Isgur and G. Karl, Phys. Rev. D23, 155 (1981).
4. D. Strottman, Phys. Rev. 18, 2716 (1978).
5. F. Dydak, F. L. Navarria, O. E. Overseth, P. Steffen et al., Nucl. Phys. B118, 1 (1977).
6. T. S. Mast et al., Phys. Rev. Lett. 21, 1715 (1968).
7. J. Colas et al., Nucl. Phys. B91, 253 (1975).
8. H. Primakoff, Phys. Rev. 31, 899 (1951).
9. A. Browman et al.,Phys. Rev. Lett. 32, 1067 (1974).
10. A. Browman et al., Phys. Rev. Lett. 33, 1400 (1974).
11. D. Berg et al., Phys. Rev. Lett. 44, 706 (1980).
12. D. Berg et al., Phys. Rev. Lett. 98B, 119 (1981).
13. S. Cihangir, et al., Submitted to Phys. Rev. Lett.
14. S. Cihangir, et al., Submitted to Phys. Rev. Lett.
15. F. Dydak, et al., Nucl. Phys. B118, 1 (1977).
16. G. Faldt, et al., Nucl. Phys. B41, 125 (1972).
17. C. Wilkin, private communication.
18. J. Lach, private communication.
19. G. E. Brown, et al., Phys. Lett. 97B, 423 (1980).
20. H. J. Lipkin, Phys. Lett. 35B, 534 (1971).
21. R. T. Deck, Phys. Rev. Lett. 13, 169 (1964); L. Stodolsky, Phys. Rev. Lett. 18, 973 (1967).
22. V. Hungerbuhler, Phys. Rev. D10, 2051 (1974).

FIGURE CAPTIONS

Fig. 1. Level diagram of low-lying S = -1,-2 resonances.

Fig. 2. Quark level occupation diagram for the Λ, Σ ground states and for the $\Sigma^*(1385)$ in the q^3 model.

Fig. 3. Quark level occupation diagram for the Ξ ground and excited states in the q^3 model.

Fig. 4. Quark level occupation diagram for the $\Lambda^*(1405)$ in the q^3 model.

Fig. 5. Quark level occupation diagrams for the $\Lambda^*(1520)$ in the q^3 model. Both singlet and octet configurations are shown.

Fig. 6. t_3 versus hypercharge display of the SU(3) baryon octet and decaplet. The I, U, and V-spin axes are as shown.

Fig. 7. Feynman diagram for Primakoff excitation.

Fig. 8. The eight Primakoff transitions that are in principle measurable at the FNAL hyperon beam facility. The incident beam required for the measurement is as shown.

Fig. 9. Primakoff total production cross sections in millibarns for neutral beam transitions are calculated using the available confinement model predictions. The dashed horizontal line indicates the magnitude of the already measured $\Lambda \cdot \gamma \rightarrow \Sigma^0$ transition. The cross sections shown are for 200 GeV/c incident momentum on a uranium target.

Fig. 10. Same as Fig. 9 except for charged beam transitions. Note that the positive beam transition uses the right-hand scale and the negative beam transitions use the left-hand scale.

TABLE I

STATE PROPERTIES AND PRINCIPLE DECAY

MODES FOR LEVELS OF INTEREST

STATE	σ_{TOT}(mb)	J^{π}	DECAY	%
Λ^{o}(1115.6)	BLW	$\frac{1}{2}^{+}$	$P\pi^{-}$	64.2
STABLE	THRSH		$n\pi^{o}$	35.8
Λ^{*}(1405)	BLW	$\frac{1}{2}^{-}$	$\Sigma\pi$	100.
$\Gamma \sim 40$	THRSH			
Λ^{*}(1520)	84	$\frac{3}{2}^{-}$	$N\bar{K}$	46.
$\Gamma = 15.5$			$\Sigma\pi$	42.
			$\Lambda\pi\pi$	10.
			$\Sigma\pi\pi$	0.9
Σ^{+}(1189)	BLW	$\frac{1}{2}^{+}$	$P\pi^{o}$	51.6
STABLE	THRSH		$n\pi$	48.4
Σ^{o}(1192)	BLW	$\frac{1}{2}^{+}$	$\Lambda\gamma$	100.
STABLE	THRSH			
Σ^{-}(1197)	BLW	$\frac{1}{2}^{+}$	$N\pi^{-}$	100.
STABLE	THRSH			
Σ^{*}(1385)	BLW	$\frac{1}{2}^{+}$	$\Lambda\pi$	88.
$\Gamma \sim 40$	THRSH		$\Sigma\pi$	12.
Ξ^{o}(1315)		$\frac{1}{2}^{+}$	$\Lambda\pi^{o}$	100.
STABLE				
Ξ^{-}(1321)		$\frac{1}{2}^{+}$	$\Lambda\pi^{-}$	100.
STABLE				
Ξ^{*}(1530)		$\frac{3}{2}^{+}$	$\Xi\pi$	100.
$\Gamma = 10.1$				

TABLE II

RADIATIVE WIDTHS IN THE MIT BAG MODEL

AND IN THE MODEL OF ISGUR AND KARL (IK)

Transition	Γ_γ (KeV) MIT Bag	IK SU(6)	IK uds	CQ
$\Lambda^*(3/2^-) \to \Sigma^*(3/2^+)$	0	0.034	0.079	--
$\Sigma(1/2^+)$	68	49	45	--
$\Lambda^*(1/2^-$	0.002	0.35	0.66	--
$\Lambda(1/2^+)$	3.40	88	122	--
$\Lambda^*(1/2^- \to \Sigma^*(3/2^+)$	0	0.24	0.23	--
$\Sigma(1/2^+)$	0	65	60	--
$\Lambda(1/2^+)$	2.8	137	164	--
$\Sigma^{*o}(3/2^+) \to \Lambda(1/2^+)$	154	243	242	274 ± 5
$\Sigma^o(1/2^+)$	14	19	19	16.8 ± 0.4
$\Sigma^{*-}(3/2^+) \to \Sigma^-(1/2^+)$	---	2.3	2.1	3.7 ± 0.4
$\Sigma^{*+}(3/2^+) \to \Sigma^+(1/2^+)$	---	103	103	106 ± 1
$\Sigma^o(1/2^+) \to \Lambda(1/2)^+$	4.50	8.4	8.8	12.1 ± 0.2
$\Xi^{*o}(3/2^+) \to \Xi^o(1/2^+)$	---	118	119	116 ± 5
$\Xi^{*-}(3/2^+) \to \Xi^-(1/2^+)$	---	2.6	2.8	$1.7 \begin{matrix} + 2.0 \\ - 1.3 \end{matrix}$

TABLE III

RADIATIVE WIDTHS IN THE MIT BAG MODEL

FOR $q^4\bar{q}$ AND q^3 ADMIXTURES

Transition	Γ (KeV) $\lvert q^4\bar{q}\rangle + \lvert q^3\rangle$	$\lvert q^4\bar{q}\rangle - \lvert q^3\rangle$
$\Lambda(3/2^-) \to \Sigma(1/2^+)$	100.0	88.0
$\Lambda(1/2^+)$	25.0	9.0
$\Lambda(1/2^-) \to \Sigma(1/2^+)$	325.0	325.0
$\Lambda(1/2^+)$	20.0	6.0

TABLE IV

EXPERIMENTAL PARAMETERS USED IN COUNT RATE ESTIMATES

Transition	F.S.	F.S.B.R.	σ_{ror} (mb)	TRCT (L_{int})	Flux (/PLS)	Events (/PLS)	Events (/day)
$\Sigma^-\gamma \rightarrow \Sigma^{-*}(1385)$	$p\pi^-\pi^-$	0.56	0.42	0.1	10^4	0.12	600
$\Sigma^+\gamma \rightarrow \Sigma^{+*}(1385)$	$p\pi^-\pi^+$	0.56	15.2	0.1	160	0.07	350
$\Xi^-\gamma \rightarrow \Xi^{-*}(1530)$	$p\pi^-\pi^-\pi^0$	0.32	0.24	0.1	200	1×10^{-3}	4
$\Lambda\gamma \rightarrow \Lambda^*(1405)$	$p\pi^-\gamma\pi^0$	0.21	04.9	0.03	5000	0.08	390
$\Lambda\gamma \rightarrow \Sigma^{0*}(1385)$	$p\pi^-\pi^0$	0.56	12.0	0.03	5000	0.51	2550
$\Lambda\gamma \rightarrow \Lambda^*(1520)$	PK^-	0.23	3.0	0.10	5000	0.17	870
$\Xi^0\gamma \rightarrow \Xi^{0*}(1530)$	$p\pi^-\pi^-\pi^+$	0.32	11.0	0.10	100	0.02	90

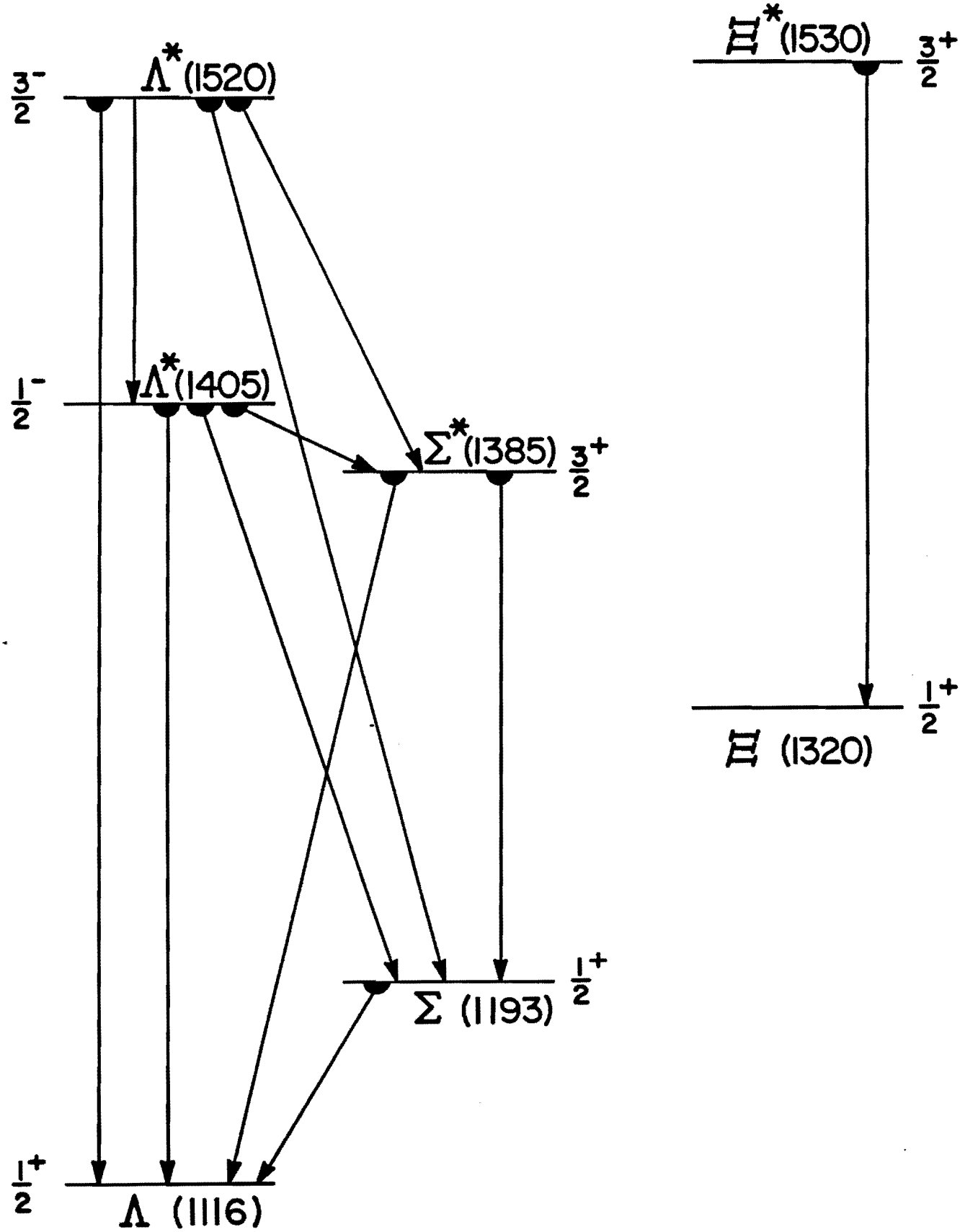
$\Xi^*(1530)$ $\frac{3}{2}^+$
$\frac{3}{2}^-$ $\Lambda^*(1520)$
$\frac{1}{2}^-$ $\Lambda^*(1405)$
$\Sigma^*(1385)$ $\frac{3}{2}^+$
$\frac{1}{2}^+$
Ξ (1320)
Σ (1193) $\frac{1}{2}^+$
$\frac{1}{2}^+$
Λ (1116)

Figure 1

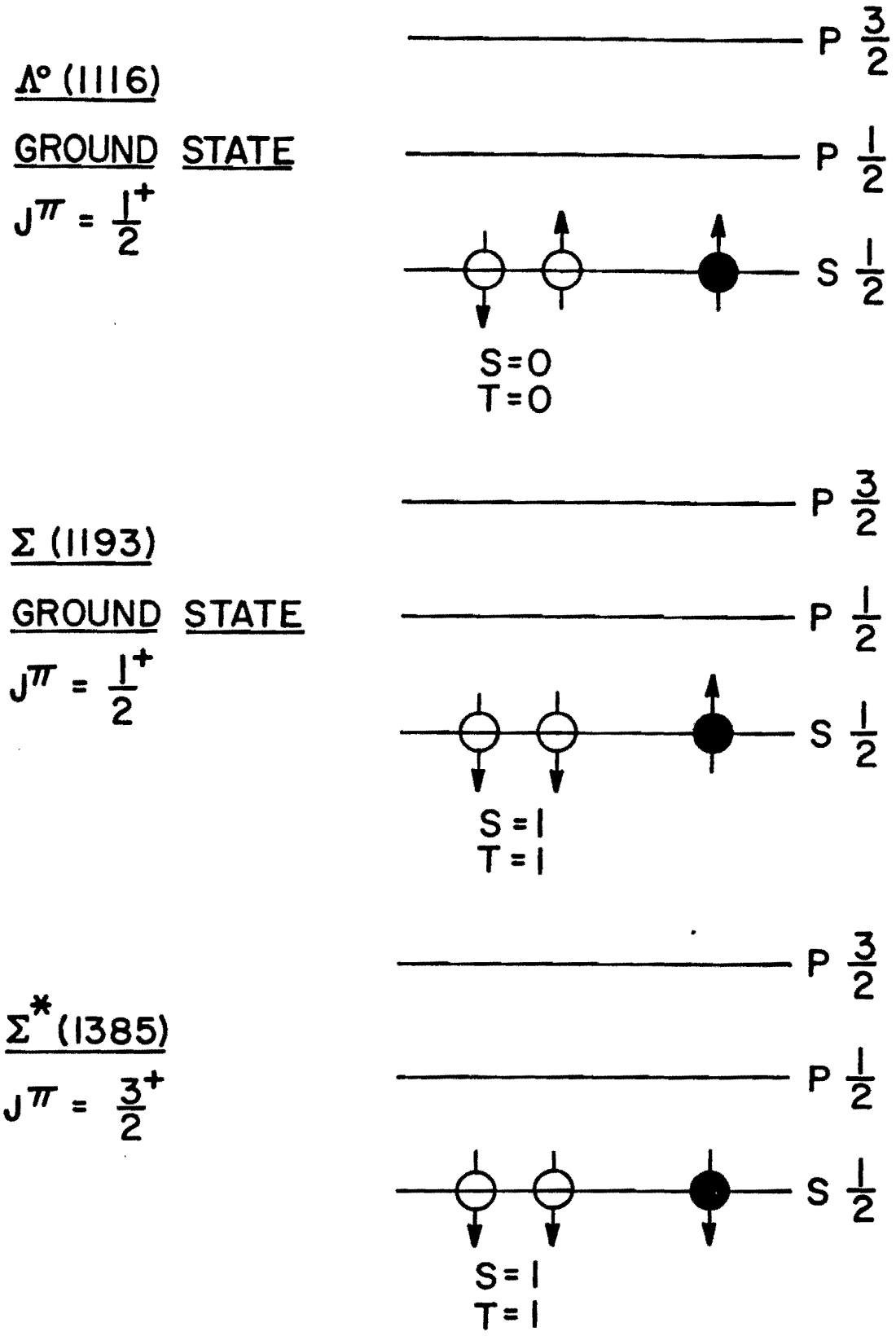
Λ° (1116)
GROUND STATE
$J^{\pi} = \frac{1}{2}^{+}$
P 3/2
P 1/2
S 1/2
S=0
T=0
Σ (1193)
GROUND STATE
$J^{\pi} = \frac{1}{2}^{+}$
P 3/2
P 1/2
S 1/2
S=1
T=1
Σ^{*} (1385)
$J^{\pi} = \frac{3}{2}^{+}$
P 3/2
P 1/2
S 1/2
S=1
T=1

Figure 2

$\Xi^*(1530)$

$J^\pi = \frac{3}{2}^+$

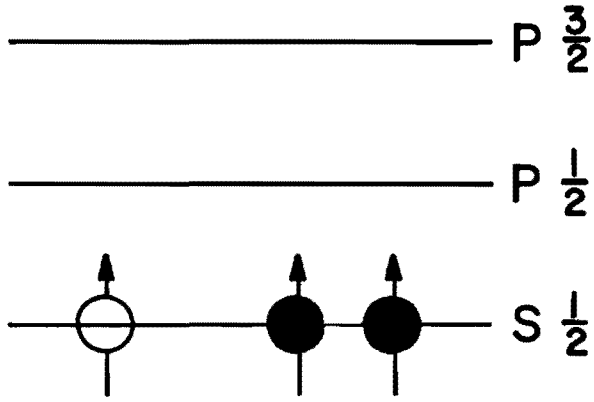

$\Xi(1320)$

GROUND STATE

$J^\pi = \frac{1}{2}^+$

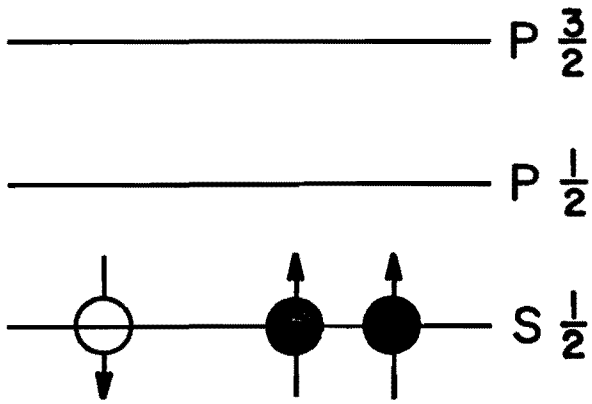

Figure 3

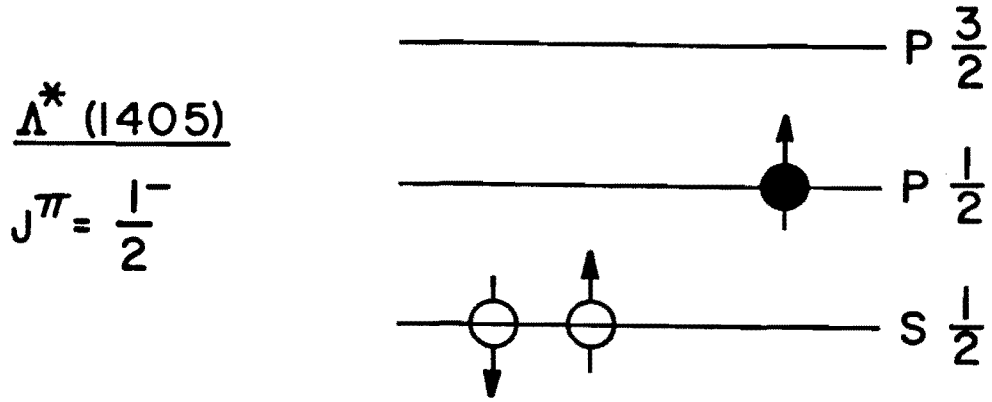

Figure 4

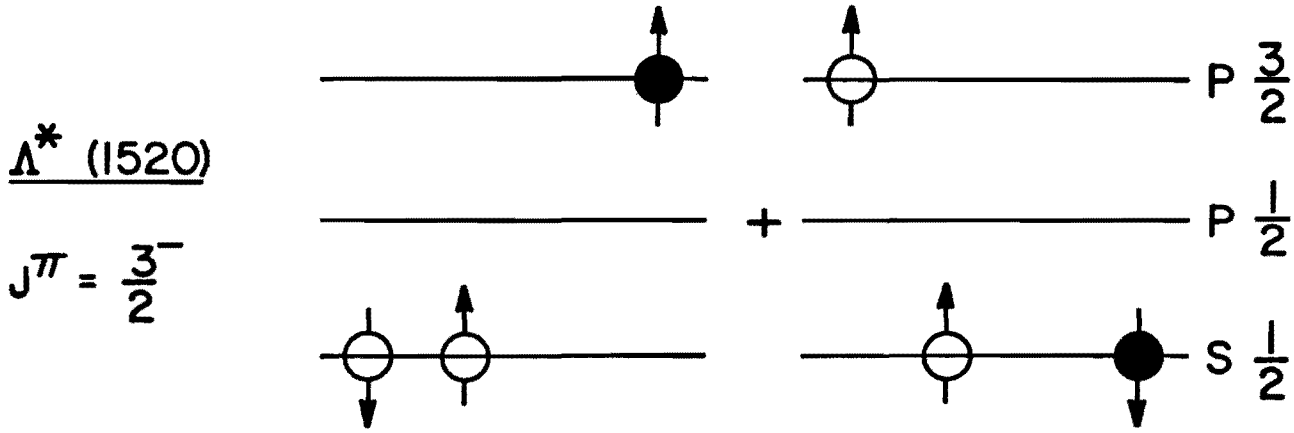

Figure 5

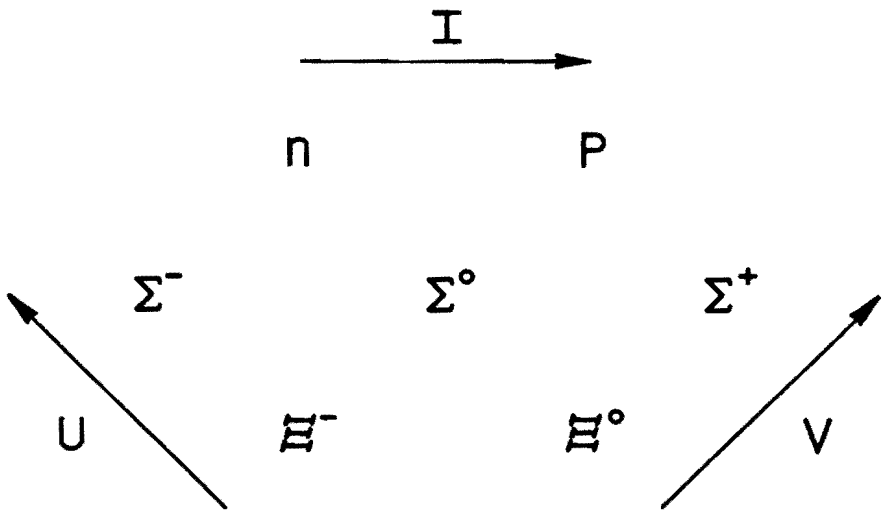

$\frac{1}{2}^+$ BARYON OCTET

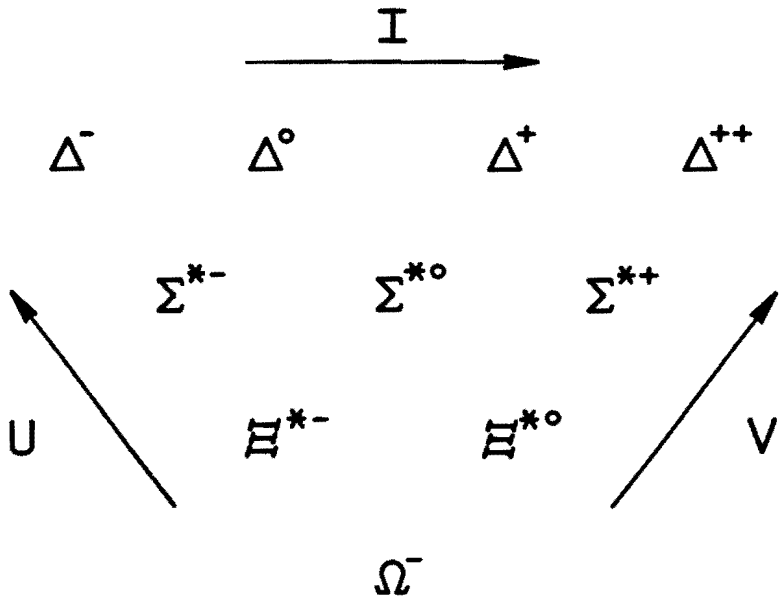

$\frac{3}{2}^+$ BARYON DECUPLET

Figure 6

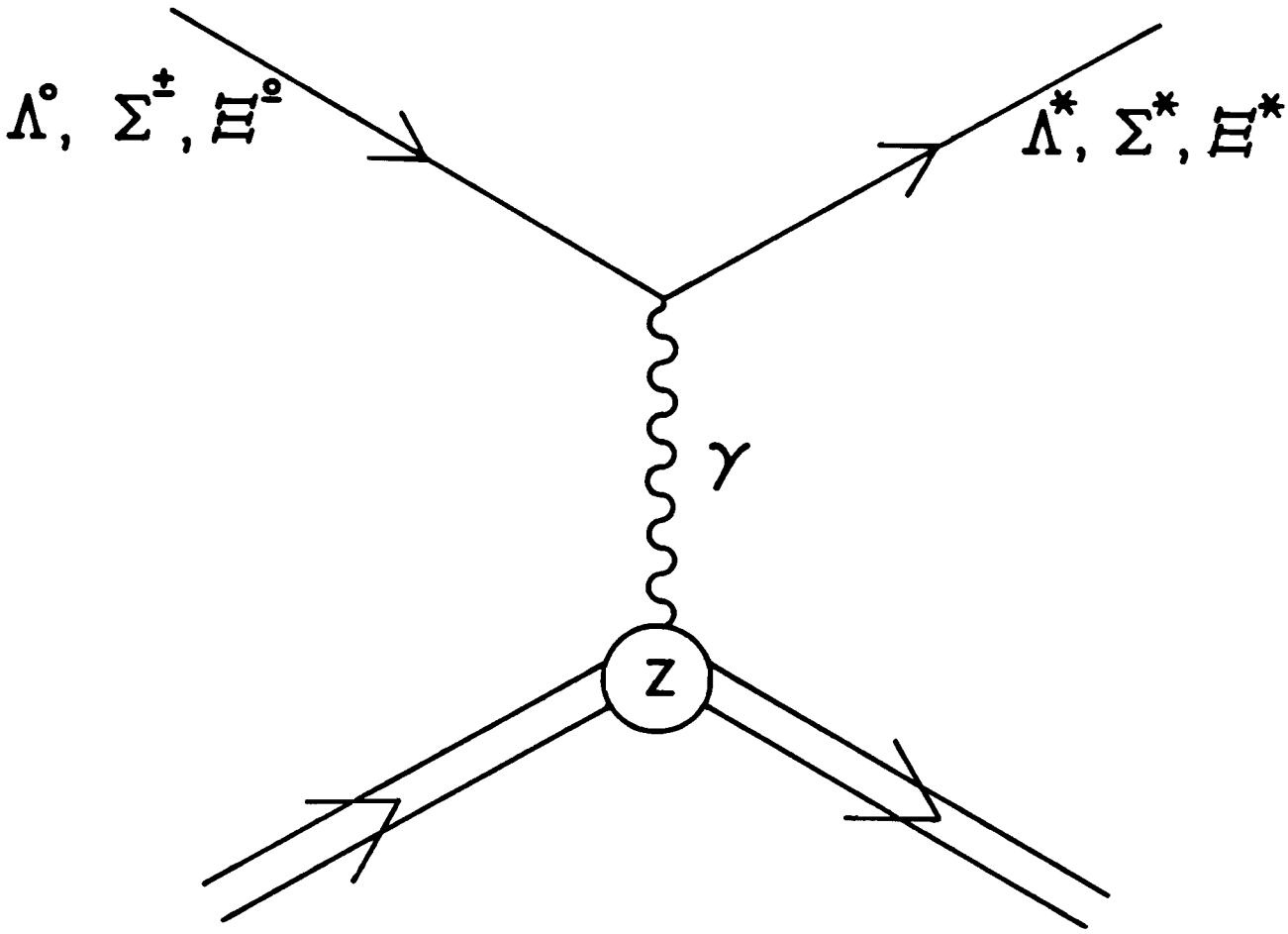

Figure 7

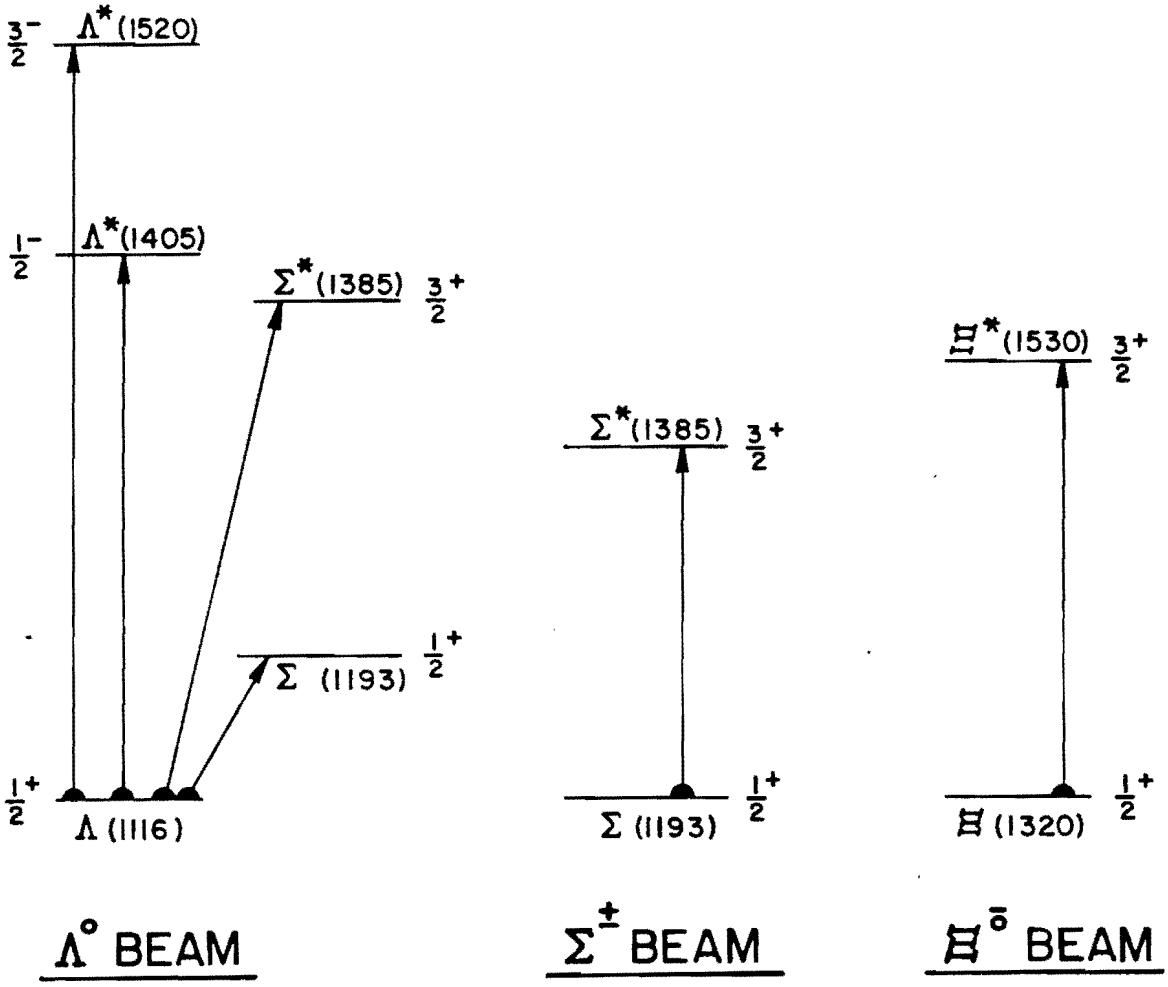
3/2⁻ Λ*(1520)
1/2⁻ Λ*(1405)
Σ*(1385) 3/2⁺
Σ (1193) 1/2⁺
1/2⁺ Λ (1116)
Λ° BEAM
Σ*(1385) 3/2⁺
Σ (1193) 1/2⁺
Σ± BEAM
Ξ*(1530) 3/2⁺
Ξ (1320) 1/2⁺
Ξ° BEAM

Figure 8

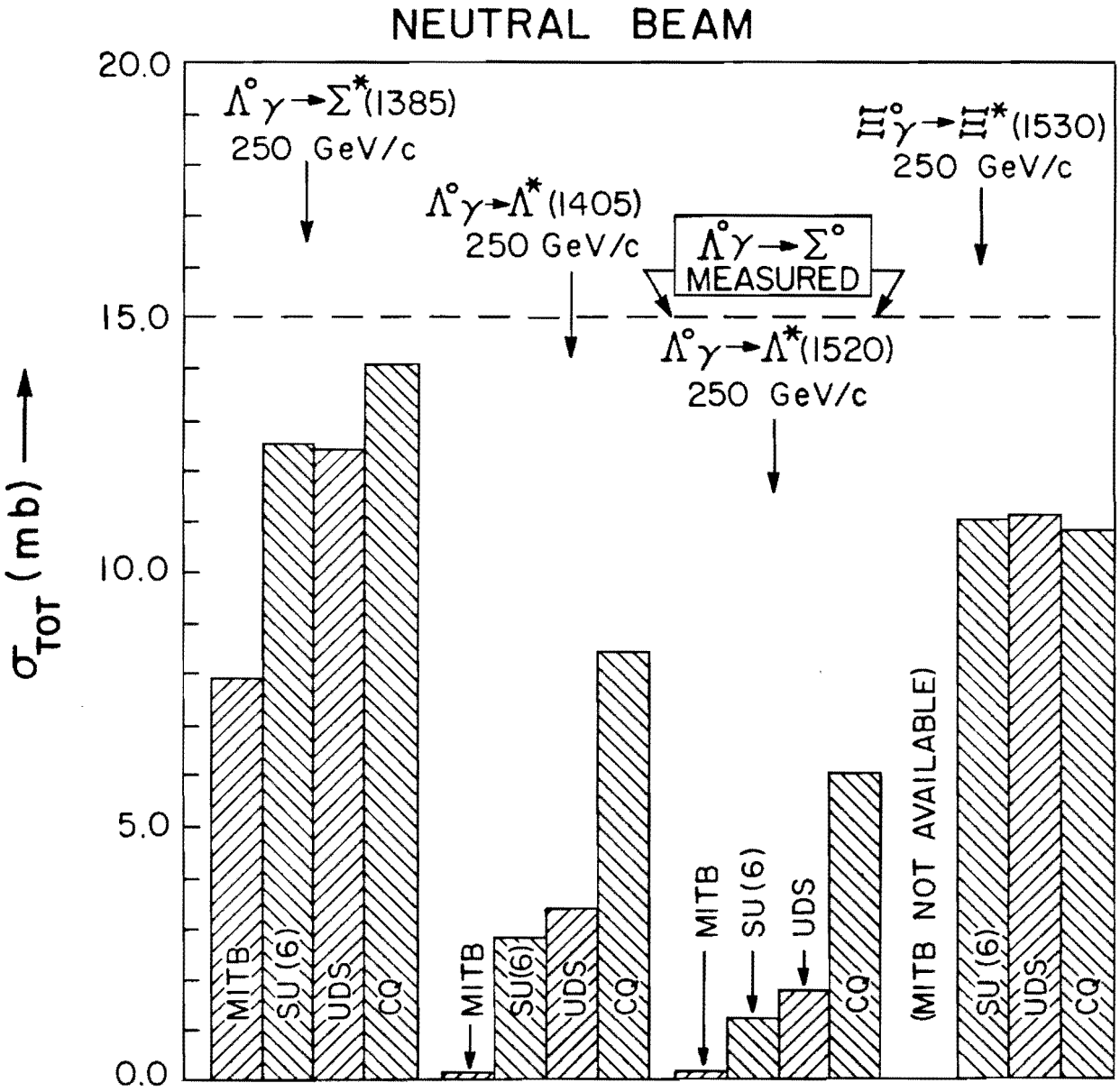
NEUTRAL BEAM
20.0
15.0
10.0
5.0
0.0
σ_{TOT} (mb)
$\Lambda^\circ\gamma \rightarrow \Sigma^*(1385)$
250 GeV/c
$\Lambda^\circ\gamma \rightarrow \Lambda^*(1405)$
250 GeV/c
$\Lambda^\circ\gamma \rightarrow \Sigma^\circ$
MEASURED
$\Lambda^\circ\gamma \rightarrow \Lambda^*(1520)$
250 GeV/c
$\Xi^\circ\gamma \rightarrow \Xi^*(1530)$
250 GeV/c
MITB
SU(6)
UDS
CQ
(MITB NOT AVAILABLE)

Figure 9

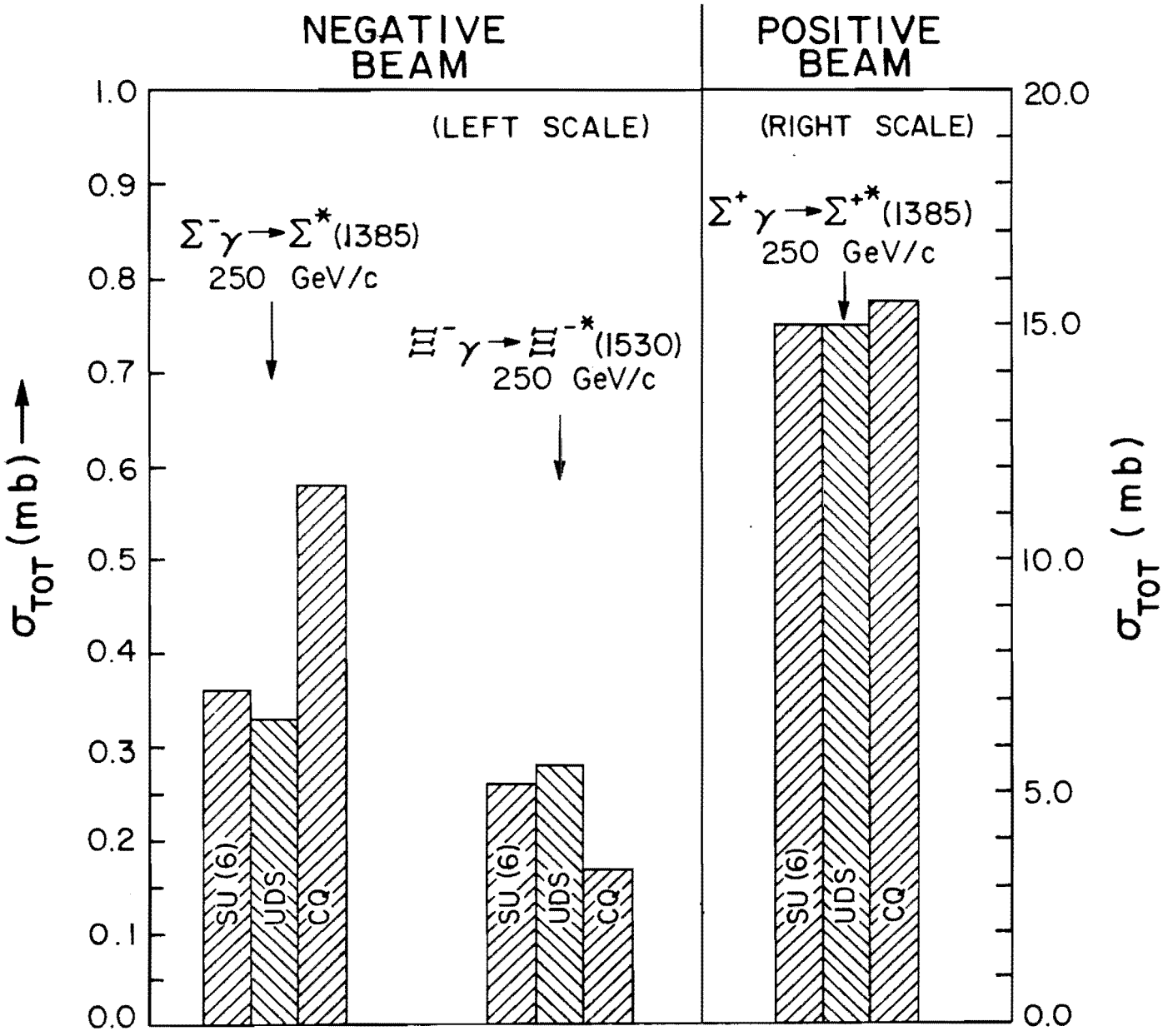
NEGATIVE BEAM
POSITIVE BEAM
(LEFT SCALE)
(RIGHT SCALE)
$\Sigma^- \gamma \rightarrow \Sigma^*(1385)$
250 GeV/c
$\Xi^- \gamma \rightarrow \Xi^{-*}(1530)$
250 GeV/c
$\Sigma^+ \gamma \rightarrow \Sigma^{+*}(1385)$
250 GeV/c
σ_{TOT} (mb)
σ_{TOT} (mb)
SU(6)
UDS
CQ
1.0
0.9
0.8
0.7
0.6
0.5
0.4
0.3
0.2
0.1
0.0
20.0
15.0
10.0
5.0
0.0

Figure 10